Using Replicator Dynamics for Analyzing fMRI Data of the Human Brain

Gabriele Lohmann* and Stefan Bohn

Abstract—**The understanding of brain networks becomes increasingly the focus of current research. In the context of functional magnetic resonance imagery (fMRI) data of the human brain, networks have been mostly detected using standard clustering approaches. In this work, we present a new method of detecting functional networks using fMRI data. The novelty of this method is that these networks have the property that every network member is closely connected with every other member. This definition might to be better suited to model important aspects of brain activity than standard cluster definitions. The algorithm that we present here is based on a concept from theoretical biology called "replicator dynamics."**

Index Terms—**Clustering, fMRI data, functional connectivity, network analysis, replicator dynamics.**

I. Introduction

In this paper, we will introduce a new approach to modeling and detecting functionally coherent networks in the human brain based on a well-known concept of theoretical biology called "replicator equations." Our approach is based on measurement data of functional magnetic resonance imagery (fMRI). In fMRI, test subjects are subjected to cognitive or sensory stimuli and are asked to respond to them while a sequence of $T2^*$-weighted magnetic resonance images are acquired. In the course of a typical fMRI experiment, several hundred or even several thousand images are recorded at a rate of about 1–2 s/image. Usually, these image sequences are then analyzed using standard statistical techniques to reveal areas in the brain that are significantly activated when a stimulus condition is contrasted against some baseline condition. The result of such an analysis is an activation map that shows the degree of statistical significance with which each pixel can be considered to be activated.

While such maps are of large value for purposes of human brain mapping, they do not reveal interdependencies between areas of activations. Therefore, the aim of this paper is to present a new approach that allows us to identify such interdependencies of brain activations and to detect functionally coherent networks within an fMRI image sequence. The basic assumption here is that during the course of an fMRI experiment, several brain regions are active and interact with each other and, thus, form a functionally coherent network. We assume that these networks can be detected by analyzing correlations between fMRI time courses. The important point to note here is that our algorithm is *not* a clustering algorithm because our concept of a coherent network differs from the traditional cluster concept.

A large number of clustering methods for a variety of application domains exist and have been described in the literature [1]. Clustering has also been applied in the present domain of application [2]–[5]. The difference between the method proposed in this work is in the definition of a cluster. Usually, a clustering is defined as a partitioning of a feature space into several components such that the elements within the same component are close to some central element and the distances between different components are large. Thus, most traditional clustering algorithms identify star-shaped topologies in which each element of the feature space is associated with one of a few central elements.

In contrast, we aim at finding networks (or clusters) that exhibit quite different coherence properties: each element of a network must be close to as many other nodes as possible. Thus, the resulting network plays a dominant role in the graph.

This requirement seems to be better suited to our domain of application: we want to identify networks of brain activity such that all members that belong to the same network interact with each other. Current knowledge about brain processes suggest that such topologies are more realistic than star-shaped topologies. In order to differentiate between those two concepts, we will subsequently use the term "network" instead of "cluster." This concept of a coherent network is close to the concept of a clique in graph theory. A clique is defined as a collection of nodes in a graph such that any two nodes are connected by an arc.

The algorithm that we propose is based on a concept well known in theoretical biology called "replicator dynamics." Replicator dynamics describe the growth of populations consisting of several species that interact with each other. Replicator dynamics have recently been used in the context of graph theory as a means of detecting maximal cliques for graph matching purposes [6].

We have adapted the concept of replicator dynamics for our purposes because it allows us to detect networks in the sense described above. In addition to supporting this new notion of a network, our method has the additional advantage of only using pairwise similarity measurements rather than an explicit measurement vector in each pixel. In our context, this is particularly advantageous as the entities that we want to process are very high-dimensional vectors of time courses. Similarity measurements of time courses can be easily obtained without loss of information, whereas time course vectors are difficult

Manuscript received November 13, 2001; revised March 6, 2002. *Asterisk indicates corresponding author.*

*G. Lohmann is with the Max-Planck-Institute of Cognitive Neuroscience, 04103 Leipzig, Germany (e-mail: lohmann@cns.mpg.de).

S. Bohn is with the Max-Planck-Institute of Cognitive Neuroscience, 04103 Leipzig, Germany.

Publisher Item Identifier S 0278-0062(02)05533-7.

to handle due to the high dimensionality. Pairwise clustering methods have been proposed by Hofmann *et al.*[7] for pattern recognition purposes, but it has not been applied to fMRI data.

Recently, independent component analysis (ICA) has been applied to perform fMRI data analysis [8]. ICA tries to decompose the image sequence into a sequence of independent components. It is related to cluster analysis in that it is also an exploratory method.

II. Mathematical Framework

The basic idea underlying our approach is that functional networks can be detected solely by analyzing pairwise similarity measurements between any two time series. Thus, we start out with a similarity matrix $W = (w_{ij})$ where w_{ij} represents a nonnegative, symmetric and real-valued similarity measurement between time courses in pixels i and j.

Our goal is to detect a maximally coherent network of pixels. We denote this network as M. The degree of coherence relative to M is defined as follows. Let $x_i \in [0, 1]$ represent the degree of membership of pixel i in M. Thus, if $i \in M$, then $x_i = 1$ and $x_i = 0$, if $i \notin M$. We also allow "fuzzy" membership values, so that x_i may attain any value in the interval [0, 1]. Let $x = (x_1, \ldots, x_n)$ with n being the number of pixels in the image. We then define the degree of coherence relative to M as $x^T W x$.

In order to detect such a maximally coherent network M, we must find a vector x that maximizes $x^T W x$ subject to $\|x\| = 1$. The network M is then defined by its membership values x. It is well known that the maximization problem $x^T W x$ is NP-hard if W has positive eigenvalues [9]. In our case, the matrix W usually represents a correlation matrix and so it has positive eigenvalues. Thus, a careful choice of an optimization procedure is needed.

We propose to use a class of dynamical systems known from theoretical biology for this purpose. This class of dynamical systems is described by the following equation:

$$\frac{d}{dt}x_i(t) = x_i(t)[(Wx(t))_i - x(t)^T W x(t)], \quad i = 1, \ldots, n.$$

where W is a similarity matrix as described above. The discrete version of the process is given by

$$x_i(t+1) = x_i(t)\frac{(Wx(t))_i}{x(t)^T W x(t)}.$$

These equations are known as *replicator equations* [10]. They are used in theoretical biology to model frequency-dependent evolution of a population containing several interacting species. They have recently been used for addressing the maximum clique problem which can also be cast into a quadratic maximization problem [11], [6].

The dynamical properties of replicator systems are described by the famous fundamental theorem of natural selection (see also, [6] and [12]).

Theorem [12, p. 15]: Let W be a nonnegative, real-valued symmetric $n \times n$ matrix. Then the function $x(t)^T W x(t)$ increases with increasing t along any nonstationary trajectory $x(t)$ under both continuous-time and discrete time replicator dynamics. Furthermore, any such trajectory converges toward a stationary point $\bar{x}$. Finally, a vector $\bar{x} \in S_n$ is asymptotically stable if and only if $\bar{x}$ is a strict local maximizer of $x^T W x$ in S_n with $S_n = \{x \in R^n | \sum x_i = 1, x_i \geq 0, i = 1, \ldots, n\}$.

The process of detecting a maximally coherent network is now straightforward. We start out with an initial vector x which is set to $x = (1/n, \ldots, 1/n)$ to avoid an initial bias. We then apply the replicator dynamical process during which the vector x evolves toward some stationary value $\bar{x}$ that maximizes $x' W x$.

Note that the maximum x may be only local and not necessarily global. The choice of the starting point determines which of the possibly many local maxima will be reached.

As initially all components x_i of of the starting vector x have the same weight, the components that will increase their weight after the first iteration are the ones that interact most closely with many other components. As the process evolves, only those components x_i will profit that interact most closely with many other high-weighted other components. Interaction with low-weighted components becomes less and less profitable. Eventually, a small set of closely interacting components will have received a large weight while the remaining components become negligible.

These components form a closely coherent network. Note that membership in such a network is a fuzzy concept: a large value of x_i indicates a high degree of membership. In order to "defuzzify" the membership concept, we define the pixel i to belong to the network if its membership value exceeds the average value, i.e., if $x_i > 1/n$.

The process terminates if it becomes stationary, i.e., if the difference between subsequent iterations becomes negligible. We determine stationarity by counting the number of voxels that change their membership status from one iteration to the next. If no membership changes occur for more than a a given number of iterations then the process is assumed to have reached stationarity. In our experiments, we assumed stationarity if memberships have remain unchanged through more than 50 iterations.

The first network detected by the algorithm consists of all pixels i whose membership values at stationarity exceeds the average, i.e., for which $x_i > 1/n$. To detect a second network, we eliminate all pixels that are members of the first network and repeat the above process. Further networks can be detected likewise. Note that the procedure is guaranteed to terminate as each time a network is detected a positive number of pixels are removed from further consideration. Note that the networks are ranked according to their degree of coherence. The first networks have a higher degree of coherence than later networks.

The above process can be recursively applied at a second level of processing as follows. Suppose a number of networks have been detected as described above. We then update the similarity matrix such that

$$w'_{ij} = \sum_{k \in N_i, l \in N_j} w_{kl}$$

with N_i being the set of pixels belonging to network i. In other words, similarity values of pixels belonging to the same network are averaged. The replicator process is then applied again using the updated similarity matrix.

III. Coherent Networks and Maximal Cliques

As mentioned earlier, replicator dynamics have been used to identify maximal cliques in undirected graphs [6]. Thus, there exists a connection between clique detection and the detection of coherent networks as proposed here. However, some differences exist as will be illustrated in this section.

The most obvious difference is of course that coherent networks as defined in this paper can be detected using any real-valued, symmetric nonnegative matrix W. It need not be a binary valued adjacency matrix representing an undirected graph. But even if W is binary-valued, some differences exist.

As was shown by Motzkin and Strauss [13] and also by Bomze [14], the detection of maximal cliques is connected to a quadratic maximization problem of the form $x^T W x$ where W is the adjacency matrix of an undirected graph. In general, local maxima of $x^T W x$ correspond to maximal cliques in the graph. However, counterexamples exist. The following example is taken from Pardalos *et al.* [15]. Let

$$W = \begin{bmatrix} 0 & 1 & 1 \\ 1 & 0 & 0 \\ 1 & 0 & 0 \end{bmatrix}$$

be an adjacency matrix representing the following graph

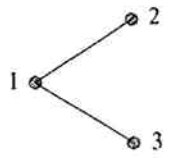

This graph has two maximal (and maximum) cliques: {1,2} and {1,3}. However, the quadratic function $x^T W x$ has many more maxima. In particular, all $(0, z, 1-z), \forall z \in [0,1]$ are global maxima. So, there is an infinite number of global maxima, but only two of them are characteristic vectors representing maximal cliques, namely $z = 0$ and $z = 0.5$ (a characteristic vector is a vector whose values are either zero or one/c, where c is the number of nodes in the clique). Therefore, not all local maxima correspond to maximal cliques. For more about this problem, see [14] and [16].

The replicator process applied to $x^T W x$ with starting vector $x = (1/3, 1/3, 1/3)$ converges to $(0.5, 0.25, 0.25)$. In our approach, the resulting fuzzy membership vector (0.5,0.25,0.25) is "defuzzyfied" to (1,0,0) giving us a single node {1} as the resulting coherent network. Clearly, this solution does not correspond to a maximal clique. In our context however, it makes perfect sense: the node "1" is the node that interacts most closely with all other nodes in the graph. Thus, the replicator dynamics yields a solution that agrees with our definition of a coherent network even though it does not represent a maximal clique.

IV. Similarity Metrics

The matrix W contains similarity values that measure the degree of dependence between time courses in any two voxels.

Let $i = 1, \ldots, n$ denote pixels in a fMRI image and let U_i denote a time course in pixel i so that $U_i = (U_{i1}, \ldots, U_{ik})$ represents a time course consisting of k time steps. Let $w_{ij} \geq 0$ denote a similarity or dependence measurement between the time courses in pixels i and j such that $w_{ij} = 0$ if the time courses are completely independent or dissimilar.

Several alternative similarity metrics are conceivable in this context. The most obvious choice is Pearson's linear correlation coefficient r that measures the degree of linear dependence. As the similarity measurements must be nonnegative, we simply take the absolute value of r. Alternatively, negative correlations may be set to zero.

Pearson's correlation statistic gives useful results provided the joint distribution of time courses U_i, U_j in pixels $i \neq j$ are approximately binormal. If this requirement is not met then the correlation results may be completely meaningless.

A similarity metric that is more robust against violations of binormality is Spearman's rank correlation. In rank correlation, the individual measurements $U_i k$ are first ranked with respect to their amplitudes and then their ranks are linearly correlated. The advantage is that the distribution of the ranks is known to be uniform, so that the interpretation of their correlation is much more robust [17, 639ff.].

Another alternative to Pearson's linear correlation coefficient is mutual information. It is defined as

$$w_{ij} = \sum_{ij} p(U_i, U_j) \log \frac{p(U_i, U_j)}{p(U_i) p(U_j)}.$$

Then $w_{ij} \geq 0$ with $w_{ij} = 0$ only if U_i and U_j are completely independent. Its primary advantage in our context is that is is capable of measuring nonlinear relationships. In addition, it always yields nonnegative values so that we do not need to take absolute values. Its disadvantage is that estimates for the joint probabilities $p(U_i, U_j)$ are hard to come by and often require some form of binning of the data.

In our experiments, we mostly used Spearman's rank correlation.

V. Intersubject Averaging

The replicator algorithm as described above requires a similarity matrix W as input. Such a matrix can be readily obtained from fMRI time series data of a single subject. However, when fMRI data from several subjects are present, we need some mechanism to combine the information from all data sets so that a single combined matrix W results.

Clearly, the data sets from all subjects must first be brought into register by aligning them with a common coordinate system. This can be achieved by using some standard registration algorithm. In our experiments, we used the algorithm described in [18].

After geometric alignment, the main idea in combining intersubject information is to obtain individual similarity matrices $W_i, i = 1, \ldots, n$ from all n subjects and then average those matrices. However, as we cannot assume normality for all W_i we first normalize them using Fisher's z transform [17, p. 637]

$$f(r) = z = 0.5 \log \left(\frac{1+r}{1-r} \right).$$

The resulting correlation values will then be approximately normal with mean

$$\mu = 0.5\left[\log\left(\frac{1+r_{\text{true}}}{1-r_{\text{true}}}\right) + \frac{r_{\text{true}}}{n-1}\right]$$

and standard deviation $\sigma(z) \approx 1/\sqrt{n-3}$.

We then average the transformed correlation matrices and perform the inverse Fisher's z transformation

$$f^{-1}(z) = r = \frac{e^{2z}-1}{e^{2z}+1}$$

to obtain a combined correlation matrix from all subjects. Thus, the combined matrix W is computed as

$$W = f^{-1}\left[\sum_{i=1}^{n} f(W_i)\right].$$

VI. Multidimensional Scaling and Replicator Dynamics

The results produced by the replicator process are difficult to validate as no "ground truth" is available. Therefore, we propose to use multidimensional scaling (MDS) as a means to visualize the similarity structure of the matrix W. In many cases, such a visualization helps to validate the segmentation results.

In MDS, the items contained in a similarity matrix are mapped into a low-dimensional space such that the similarity values are transformed as nearly as possible into Euclidean distance values [19], [20]. Usually, the MDS map has two or three dimensions.

More precisely, let $W = (w)_{ij}$ be a similarity matrix that represents pairwise similarities between items $i, j = 1, \ldots, n$. In MDS, these items are placed into a low-dimensional map such that if any two item i, j are similar, then their Euclidean distance within the map should be small and *vice versa*. The placement of the items is an optimization problem. MDS yields good results provided the dimension of the MDS map agrees with the intrinsic dimensionality of the data.

In our case, we use MDS to visualize the results of our network analysis. For this purpose, both MDS and the replicator process are based on the same similarity matrix and the labeling that the replicator process produces is visualized in the MDS map. Each voxel $i = 1, \ldots, n$ is represented by a mark in the MDS map such that any two voxels i, j whose time courses are similar are placed in proximity in the MDS map. Some examples are shown in Section IX.

MDS has been applied to the investigation of cortical activations by a number of researchers before. Young *et al.* [21] have used MDS mostly for investigating EEG signals, whereas Tagaris *et al.* [22] and Friston *et al.* [23] have used MDS in an fMRI context.

VII. Replicator Dynamics and Principal Component Analysis

The replicator process yields a succession of networks with the first networks being the most dominant ones and later networks becoming less and less coherent. Thus, the process is intrinsically hierarchical.

As a result, networks further down the line become of lesser interest to the researcher. This is an effect that may be undesirable in many cases. Therefore, we will propose a modification of our original approach that often helps to illicit lower order networks.

The main idea is to apply the replicator process to successively reduced versions of W. These reductions result from a principal component analysis of W and a removal of high-order components. More precisely, the modified algorithm is defined as follows.

The first network is detected exactly as described before using matrix W. To detect a second network, W is decomposed into

$$W = P_1^T D_1 P_1$$

with D_1 a diagonal matrix containing eigenvalues $\lambda_1, \ldots, \lambda_n$ and P_1 the matrix of eigenvectors of W. Since W is real-valued and symmetric, such a decomposition will always exist.

Now remove the first principal component by setting P_2 to P_1 and D_2 to D_1 with $\lambda_1 = 0$ and let

$$W_2 = P_2^T D_2 P_2.$$

The second network is detected by applying the replicator process to matrix W_2. All subsequent networks $k = 2, \ldots, K$ are obtained by applying the replicator process to

$$W_k = P_k^T D_k P_k$$

with the first k eigenvalues removed.

Note that in our original algorithm, voxels that were identified to belong to some network are removed from further analysis and can therefore not be part of a lower order network. This is not the case in this modified approach. Here, all voxels participate in the replicator dynamic and can in principle be part of several networks. However, as the principal components are orthogonal, this will rarely happen in practice. Rather, this modified algorithm yields networks that are orthogonal to each other. As in the original method, the first networks will still be dominant in the sense that their members show stronger coherence properties. In Section IX, some experimental results will illustrate this concept.

VIII. Replicator Dynamics and Kohonen Maps

Instead of applying the replicator dynamics directly to fMRI raw data, it is also possible to pre-cluster the data and apply the process to time courses that represent cluster centers. A method of pre-clustering that is particularly useful in this context are Kohonen maps [24]. Kohonen maps have previously been used for clustering fMRI time series by Fischer *et al.* [25] and Ngan *et al.* [26].

The basic principle in Kohonen mapping is the following. We begin by fixing a dimension and a lattice for the Kohonen map and initialize its nodes. For instance, the map may be a two-dimensional (2-D) lattice consisting of 11×11 grid points (nodes). These nodes represent cluster centers. We then randomly select an fMRI time series and find the node in the lat-

tice to which it is closest. This node is then moved toward the selected time series. Neighboring nodes are moved elastically along. This process is continued until some stopping criterion is satisfied.

IX. Experiments

The replicator algorithm was applied to data from two fMRI experiments. The experiments illustrate various modes in which the replicator process can be applied. In the first experiment, it is applied to all pixels belonging to the visual cortex that was activated in this case.

In the second experiment, the replicator process is only applied to maxima within the z map so that each activation area is represented by one item in the similarity matrix.

In the following, each of these experiments is described in detail.

A. Experiment 1

Two test subjects participated in our first experiment. Both were healthy volunteers who gave informed consent. The image data were acquired at a 3T Bruker 30/100 Medspec MRI scanner using a gradient recalled EPI sequence (TR = 1000 ms, TE = 40 ms, and flip angle = 40). Three fMRI slices were recorded each with a thickness of 5 mm, an interslice distance of 2 mm and a field of view (FOV) of 19.2 cm. The image matrix of contained 64×64 pixels. 300 time steps corresponding to a recording time of 5 min were acquired.

During the experiment, the subjects were subjected to visual stimuli. The experiment was designed such that baseline trials and stimulation trials alternated. During the stimulation trials, the subjects saw a pattern of rotating L-shaped figures and a fixation cross in the center. The subjects were asked to fixate the cross and press a button whenever the appearance of the cross changed. During the baseline trials only the fixation cross was visible.

The fMRI data were preprocessed using a temporal highpass filter so that baseline drifts were eliminated. In addition, a spatial Gaussian smoothing filter with a standard deviation of $\sigma = 0.8$ was applied. A standard statistical analysis using the "Lipsia"-software [18] was applied to identify those brain regions that were activated by the visual stimuli.

Experiment 1a—Standard Replicator Dynamics: In a first test, the replicator dynamic was applied to the preprocessed data. Only pixels showing a significant activation were used for the network analysis. In subject A, 665 pixels were activated so that a 665×665 similarity matrix W was used. We used Spearman's rank correlation as a similarity metric. In subject B, 595 pixels were activated resulting in a 595×595 matrix W. The results of the analysis are shown in Fig. 1.

Experiment 1b—PCA and Replicator Dynamics: In a second test, a combination of principal component analysis and replicator dynamics as described in Section VII was applied. The result is shown in Fig. 2. Note that a pattern similar to the one of experiment 1a emerges. However, fewer networks are detected.

Experiment 1c—Kohonen Networks, MDS and Replicator Dynamics: Finally, we applied the Kohonen clustering prior to the network analysis using the approach described by Fischer *et al.* [25]. A 2-D Kohonen net consisting of an 11×11 lattice was generated and linear correlations were computed between any two nodes on the lattice. Thus, the similarity matrix W contained 121×121 entries representing the 121 cluster centers.

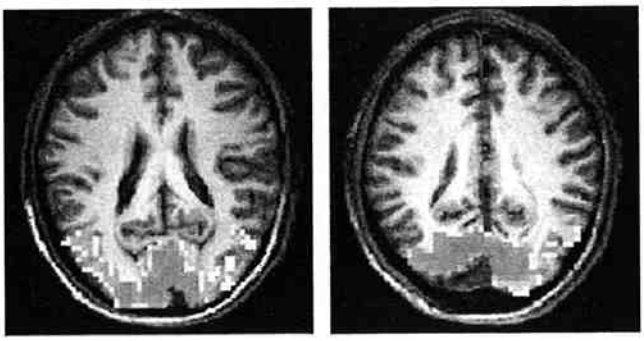

Fig. 1. Experiment 1a. The left image shows subject A, the right image shows subject B. The networks are color coded with the most prominent network appearing in red, less prominent networks appear in yellow and the least prominent networks appear in white. The red areas in both subjects belong to the primary visual cortex (V1/V2).

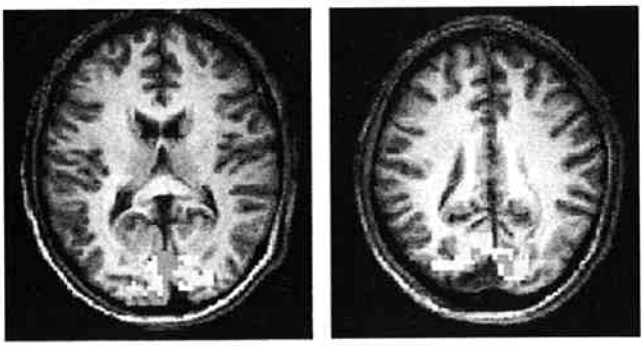

Fig. 2. Experiment 1b. The input data were the same as in experiment 1a However, this time the principal component approach as described in section VI was used. The network belonging to the first PCA is shown in red, the network belonging to the second PCA is shown in yellow. Four networks were detected.

The replicator process was then applied to the matrix W. The results are shown in Fig. 3. To better asses the correctness of the labeling, the results are additionally visualized in a 2-D MDS map (Fig. 3). Note that the MDS map reflects the topology-preserving property of the Kohonen clustering.

B. Experiment 2: Maxima of z-map

Four subjects participated in our second experiment. As before, that data were acquired at a 3T Bruker 30/100 Medspec MRI scanner using a gradient recalled EPI sequence with TR = 1500 ms, TE = 40 ms, flip angle = 40, 19.2-cm FOV. Sixteen fMRI slices with a thickness of 5 mm and an interslice distance of 2 mm were recorded. Each slice contained 64×64 pixels. The fMRI time series data contain 720 time steps corresponding to a recording time of 18 min.

The experimental design was an implementation of the so-called "color-word matching Stroop paradigm" [27]. The Stroop interference task [28] requires a person to respond to specific dimensions of a stimulus while suppressing a competing stimulus dimension. Subjects were presented two words (e.g., GREEN written in blue ink; BLUE written in black ink) and they had to match the color of the top word with the

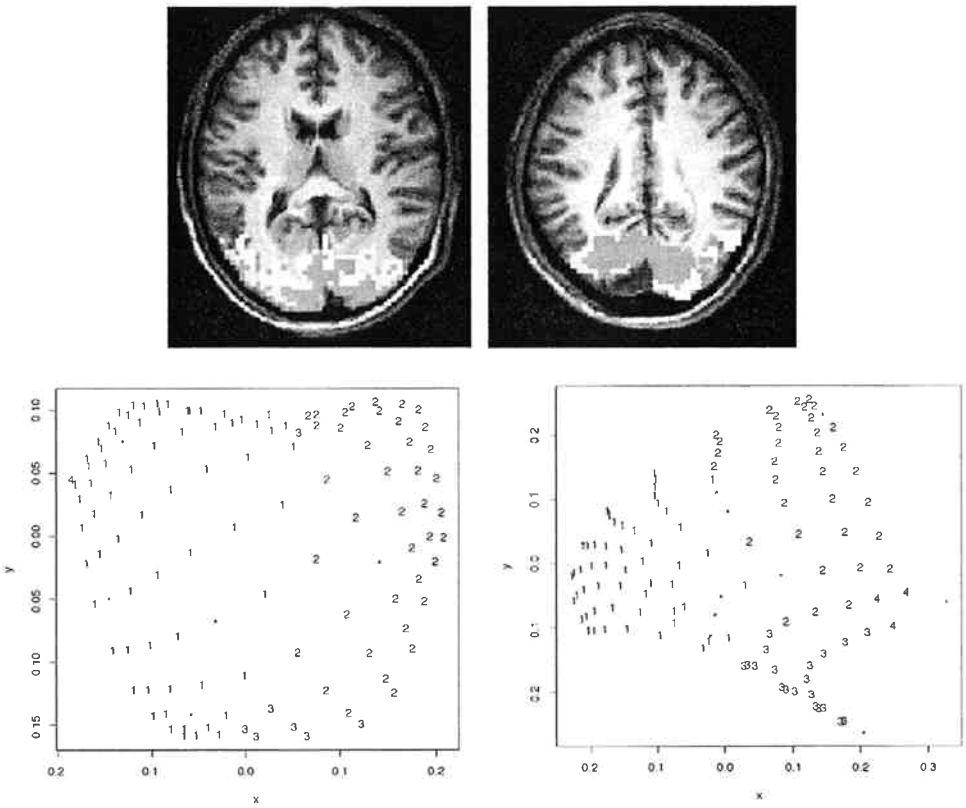

Fig. 3. Experiment 1c. The input data were the same as in experiments 1a,b. The data were pre-clustered using a Kohonen mapping. The top row shows the result of the network analysis. The bottom row shows the corresponding MDS maps.

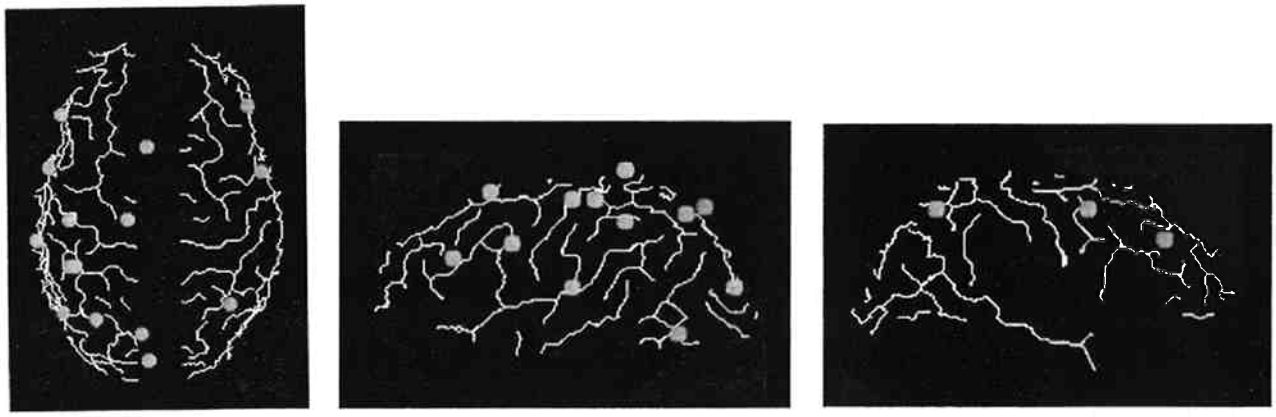

Fig. 4. Experiment 2. Local maxima of the z map were used for the replicator process. They are displayed here as colored dots against a line representation of the sulci. Three networks were detected: items belonging to the first (most prominent) network are shown in blue, the second most prominent network is shown in green and the least prominent network is shown in red.

meaning of the bottom word (Does the color of the top word correspond with the meaning of the bottom word?). Varying the dimension of the top word (neutral, congruent or incongruent words to the presented color) allows for the investigation of interference effects. The words were randomly presented every 6 s on average. Each condition was repeated 30 times.

As in the first experiment, we applied a standard statistical processing for each dataset resulting in one contrast image/subject in which all experimental conditions were contrasted against a baseline condition. A one-sample t-test across all contrast images yielded a multisubject z map (statistical parametric map). All data sets had been geometrically aligned beforehand.

We computed 16 local maxima within this multisubject z map where a pixel was defined to be a local maximum if its z value was maximal within a radius of 7 mm and if the z value exceeded a threshold of $z = 8.0$.

For each of the four subjects, a 16×16 similarity matrix W was computed using Spearman's rank correlation as a similarity metric. The correlation values were obtained at the locations of the local maxima of the z map. The four resulting correlation matrices W_i, $i = 1, \ldots, 4$ were normalized using Fisher's z transformation and then averaged as described in Section V. The replicator dynamic was applied to the averaged 16×16 matrix W. Three networks were detected. In Fig. 4 they are shown

as colored dots against a sulcal line representation that was extracted using the algorithm described in [29].

The most dominant network that the algorithm detected is known as the fronto-parietal network involving the inferior-frontal and intra-parietal sulcus as well as the pre-SMA. The second network (shown in green) corresponds to primary sensory-motor areas and the least significant network (shown in red) is an assembly of remaining areas.

Note that the degree of coherence as expressed by $x'Wx$ decreases from the first to the third network. For the first network, it equalled $x'Wx = 0.37$; for the second, it was $x'Wx = 0.29$; and for the third, it was $x'Wx = 0.24$. Therefore, the third network might perhaps not truly represent a functionally meaningful network.

X. Discussion

We have presented a new approach to detecting functional networks in fMRI time series. Our definition of a network resembles that of a clique in a graph. Therefore, it captures entities that are different from those targeted in standard clustering algorithms. This new concept seems to be better suited to the present domain of application.

Another advantage over many traditional clustering methods is that we only use pairwise similarity values. Thus, weavoid problems inherent in high dimensionality. Furthermore, our method requires no prior information about the number of networks, about their locations in space or their statistical distributions.

A potential problem of the approach may be the restriction to nonnegative similarity values. At present, we simply set negative values to zero, or use their absolute values. In practice, this approach seldom causes serious problems. The time courses used in the experiments reported here were all positively correlated as they were all influenced by similar experimental conditions.

The algorithm has several areas of application. First, it may be used for explorative bottom-up preprocessing of the data so that dominant networks and perhaps also artifacts are detected prior to further statistical processing. Networks can, thus, be identified without any prior knowledge about the experimental design. Some networks may even be independent of the experimental design. They would remain undetected in standard statistical processing techniques.

The algorithm may also be helpful in detecting functional network where no design information is available. For instance, one might want to mask all pixels in an image that are activated within one particular experimental condition. Our algorithm might then be used to further subdivide this mask into pixels belonging to several coherent networks that are activated under the same experimental condition. We are currently investigating further domains of application.

However, the algorithm is vulnerable to physiological effects in the data. In a number of recent publications, large temporal shifts between time series measured in distant voxels was observed. For instance, in [30] temporal displacements of up to 3 s were noted between time series of voxels within the visual cortex. Such displacements cannot be solely due to cognitive effects. Rather, we must assume that some physiological influences play a role. Clearly, these temporal shifts might distort our correlation matrices.

This problem hampers not only our replicator procedure. Rather, any algorithm that is based upon correlations between fMRI time series is potentially threatened by such noncognitive effects in the data. For instance, methods based upon PCA [31], [32], ICA [8], or structural equation modeling [33], [34] all face the same problem.

Acknowledgment

The authors would like to thank Dr. T. Mildner and Dr. S. Zysset for providing the fMRI data. They would also like to thank Dr. V. Jirsa, Florida Atlantic University, Boca Raton FL, for his very helpful suggestions regarding the principal component analysis.

References

[1] R. O. Duda and P. E. Hart, *Pattern Classification and Scene Analysis*. New York: Wiley, 1973.

[2] C. Goutte, P. Toft, E. Rostrup, F. Nielsen, and L. K. Hansen, "On clustering fMRI time series," *NeuroImage*, vol. 9, pp. 298–310, 1999.

[3] A. Baume, F. T. Sommer, M. Erb, D. Wildgruber, B. Kardatzki, G. Palm, and W. Grodd, "Dynamical cluster analysis of cortical fMRI activation," *NeuroImage*, vol. 9, pp. 477–489, 1999.

[4] R. Baumgartner, C. Windischberger, and E. Moser, "Quantification in functional magnetic resonance imaging: Fuzzy clustering vs. correlation analysis," *Magn. Reson. Imag.*, vol. 16, no. 2, pp. 115–125, 1998.

[5] K.-H. Chuang, M.-J. Chiu, and C. C. Lin, "Model-free functional MRI analysis using Kohnen clustering neural network and fuzzy c-means," *IEEE Trans. Med. Imag.*, vol. 18, pp. 1117–1128, Dec. 1999.

[6] M. Pellilo, K. Siddiqi, and S. W. Zucker, "Matching hierarchical structures using association graphs," *IEEE Trans. Pattern Anal. Machine Intell.*, vol. 21, pp. 1105–1119, Nov. 1999.

[7] T. Hofmann and J. M. Buhmann, "Pairwise data clustering by deterministic annealing," *IEEE Trans. Pattern Anal. Machine Intell.*, vol. 19, pp. 1–14, Jan. 1997.

[8] M. J. McKeown, M. J. S. Makeig, G. G. Brown, T. P. Jung, S. S. Kindermann, A. J. Bell, and T. F. Sejnowski, "Analysis of fMRI data by blind separation into independent spatial components," *Human Brain Mapping*, vol. 6, no. 3, pp. 160–188, 1998.

[9] P. M. Pardalos and S. A. Vavasis, "Quadratic programming with one negative eigenvalue is NP-hard," *J. Global Optimizat.*, vol. 1, no. 1, pp. 15–22, 1991.

[10] P. Schuster and K. Sigmund, "Replicator dynamics," *J. Theoretical Biol.*, vol. 100, pp. 533–538, 1983.

[11] I. M. Bomze, M. Pellilo, and V. Stix, "Approximating the maximum weight clique using replicator dynamics," *IEEE Trans. Neural Networks*, vol. 11, pp. 1228–1241, June 2000.

[12] J. Hofbauer and K. Sigmund, *The Theory of Evolution and Dynamical Systems*. Cambridge, U.K.: Cambridge Univ. Press, 1988.

[13] T. S. Motzkin and E. G. Strauss, "Maxima for graphs and a new proof of a theorem of Turan," *Can. J. Math.*, vol. 17, pp. 533–540, 1965.

[14] I. M. Bomze, "Evolution toward the maximum clique," *J. Global Optimizat.*, vol. 10, pp. 143–164, 1997.

[15] P. M. Pardalos and A. T. Philipps, "A global optimization approach for solving the maximum clique problem," *Int. J. Comput. Math.*, vol. 33, pp. 209–216, 1990.

[16] M. Pellilo and A. Jagota, "Feasible and infeasible maxima in a quadratic program for maximum clique," *J. Artif. Neural Networks*, vol. 2, no. 4, pp. 411–420, 1995.

[17] W. H. Press, S. A. Teukolsky, W. T. Vetterling, and B. P. Flannery, *Numerical Recipes in C*, 2 ed, U.K.: Cambridge Univ. Press, 1992.

[18] G. Lohmann, K. Müller, V. Bosch, H. Mentzel, S. Hessler, L. Chen, and D. Y von Cramon, "Lipsia—A new software system for the evaluation of functional magnetic resonance images of the human brain," *Computerized Med. Imag. Graph.*, vol. 25, no. 6, Nov./Dec. 2001.

[19] W. S. Torgerson, *Theory and Methods of Scaling*. New York: Wiley, 1958.

[20] G. A. F. Seber, *Multivariate Analysis*. New York: Wiley, 1984.
[21] M. P. Young, J. W. Scannell, and G. Burns, *The Analysis of Cortical Connectivity*. Berlin, Germany: Springer Verlag, 1995.
[22] G. A. Tagaris, W. Richter, S. G. Kim, G. Pellizzer, P. Andersen, K. Ugurbil, and A. P. Georgopoulos, "Functional magnetic resonance imaging of mental rotation and memory scanning: A multidimensional scaling analysis of brain activtion patterns," *Brain Res. Rev.*, vol. 26, no. 2–3, pp. 106–112, 1998.
[23] K. J. Friston, C. D. Frith, P. Fletcher, P. F. Liddle, and R. S. J. Frackowiak, "Functional topography: Multidimensional scaling and functional connectivity in the brain," *Cerebral Cortex*, vol. 6, pp. 156–164, 1996.
[24] T. Kohonen, *Self-Organizing Maps*. New York: Springer Verlag, 1995.
[25] H. Fischer and J. Hennig, "Neural network-based analysis of MR time series," *Magn. Reson. Med.*, vol. 41, pp. 124–131, 1999.
[26] S.-C. Ngan and X. Hu, "Analysis of functional magnetic resonance imaging data using self-organizaing mapping with spatial connectivity," *Magn. Reson. Med.*, vol. 41, pp. 939–946, 1999.
[27] S. Zysset, K. Müller, G. Lohmann, and D. Y. v. Cramon, "Color-word matching stroop task: Separating interference and response conflict," *Neuroimage*, vol. 13, pp. 29–36, 2001.
[28] J. Stroop, "Studies of interference in serial verbal reactions," *Exp. Psych.*, vol. 18, pp. 643–662, 1935.
[29] G. Lohmann, "Extracting line representations of sulcal and gyral patterns in MR images of the human brain," *IEEE Trans. Med. Imag.*, vol. 17, pp. 1040–1048, Dec. 1998.
[30] K. Müller, G. Lohmann, and D. Y. von Cramon, "On multivariate sprectral analysis of fMRI time series," *Neuroimage*, vol. 14, pp. 347–356, 2001.
[31] K. J. Friston, "Functional and effective connectivity in neuroimaging: A synthesis," *Human Brain Mapping*, vol. 2, pp. 56–78, 1994.
[32] E. T. Bullmore, S. Rabe-Hesketh, R. G. Morris, S. C. R. Williams, L. Gregory, J. A. Gray, and M. J. Brammer, "Functional magentic resonance image analysis of a large-scale neurocognitive network," *NeuroImage*, vol. 4, pp. 16–33, 1996.
[33] C. Büchl and K. J. Friston, "Modulation of connectivity in visual pathways by attention: Cortical interactions evaluated with structural equation modeling and fMRI," *Cerebral Cortex*, vol. 7, no. 8, pp. 768–778, Dec. 1997.
[34] K. A. Bollen, *Structural Equation Models With Latent Variables*. New York: Wiley, 1989.